Geochemistry Geophysics Geosystems G3
AN ELECTRONIC JOURNAL OF THE EARTH SCIENCES
Published by AGU and the Geochemical Society

Article
Volume 9, Number 3
27 March 2008
Q03025, doi:10.1029/2007GC001892
ISSN: 1525-2027

Germanium in mid-ocean ridge flank hydrothermal fluids

C. Geoffrey Wheat
Global Undersea Research Unit, University of Alaska Fairbanks, P.O. Box 475, Moss Landing, California 95039, USA (wheat@mbari.org)

James McManus
College of Oceanic and Atmospheric Sciences, Oregon State University, 104 Ocean Administration Building, Corvallis, Oregon 97331, USA (mcmanus@coas.oregonstate.edu)

[1] We present concentrations of germanium and silicon in sediment pore waters, basaltic formation fluids, and bulk sediment from three ridge flank hydrothermal systems (RFHS). Basaltic formation fluids from warm (>30°C) RFHS have much higher Ge concentrations and Ge:Si molar ratios than overlying sediment pore waters, requiring seawater-basalt reactions to dominate Ge concentrations in basaltic formation fluids. In contrast to warm RFHS, cool (~20°C) RFHS have similar Ge concentrations in basal sediment pore waters and underlying basaltic formation fluids, implying that there is little net exchange between these two fluid reservoirs. Despite this low net exchange, Ge:Si molar ratios in basaltic formation fluids are elevated compared to seawater and overlying sediment pore waters, implying that seawater-basalt reactions must influence Ge and Si cycling. Such seawater-basalt reactions are likely associated with secondary clay formation because increases in Ge concentration scale with Mg loss from basaltic formation fluids. Processes that control Ge cycling in cold (3–10°C) RFHS are poorly constrained because our data are restricted to sediment pore waters that have been overprinted by diagenetic reactions and possibly sampling artifacts. Although net Ge fluxes from RFHS prevail over a wide temperature range, a refined estimate for the global RFHS Ge flux is currently not possible without data from cold RFHS springs or basaltic formation fluids because cold RFHS transport most of the convective heat and crustal fluid to the oceans.

Components: 10,490 words, 7 figures, 3 tables.

Keywords: ridge flank; hydrothermal; germanium; silica; geochemical cycles; sediment.

Index Terms: 0450 Biogeosciences: Hydrothermal systems (1034, 3017, 3616, 4832, 8135, 8424); 3021 Marine Geology and Geophysics: Marine hydrogeology; 0408 Biogeosciences: Benthic processes (4804).

Received 10 November 2007; **Accepted** 23 January 2008; **Published** 27 March 2008.

Wheat, C. G., and J. McManus (2008), Germanium in mid-ocean ridge flank hydrothermal fluids, *Geochem. Geophys. Geosyst.*, *9*, Q03025, doi:10.1029/2007GC001892.

1. Introduction

[2] Germanium inputs to the oceans are dominated by mid-ocean ridge hydrothermal and riverine processes [e.g., *Froelich and Andreae*, 1981; *Froelich et al.*, 1985, 1992; *Mortlock et al.*, 1993]. During high-temperature (~350°C) seawater-basalt reactions in hydrothermal systems, Ge and Si are extracted from basalt [e.g., *Froelich et al.*, 1985; *Mortlock et al.*, 1993]. This process results in a fluid with elevated Ge and Si concentrations rela-

tive to bottom seawater and a Ge:Si molar ratio that exceeds source materials. These sources include basaltic crust with a ratio of 2.6 μmol/mol [*de Argolla and Schilling*, 1978] and possibly overlying sediment, which contains diatoms with a present-day ratio of ~1 μmol/mol [*Shemesh et al.*, 1989; *Lin and Chen*, 2002].

[3] Lower-temperature hydrothermal processes on ridge flanks are also a source of Ge to the oceans, providing ~10% of the Ge flux to the oceans [*Wheat and McManus*, 2005]. This estimate is based on data from one ridge flank hydrothermal system (RFHS) located at the Baby Bare outcrop where springs vent altered hydrothermal fluids from the underlying basalt. These fluids have reacted with basaltic crust and have been altered by diffusive exchange with overlying sediment pore water prior to venting from the crust. These initial data from warm (>60°C) RFHS are tantalizing; however, the source for this Ge and the mechanism for generating the high Ge:Si molar ratio is unknown. Furthermore, most (82%) of the global convective heat loss and most (99%) of the hydrothermal water flux through the oceanic crust occurs at much lower temperatures [*Stein and Stein*, 1994; *Wheat et al.*, 2003a]. Thus, even a small chemical anomaly associated with cool or cold RFHS can result in a flux that is significant to the oceanic Ge budget.

[4] Our initial conclusions present the need for more data from a wider array of RFHS to constrain reaction mechanisms and geochemical processes, thereby providing a better estimate of Ge fluxes [*Wheat and McManus*, 2005]. This paper builds upon this earlier work by presenting new data that allow us to distinguish between sediment and basaltic sources for Ge and providing additional constraints for reactions within basaltic crust. We present data from sediment pore waters, fluids from basaltic crust (herein referred to as basaltic formation fluids), and bulk sediment analysis collected from three RFHS; the eastern flanks of the Juan de Fuca Ridge (JFR), Cocos Plate, and the southern East Pacific Rise (EPR) (Figure 1). The temperature at the sediment-basalt contact in these RFHS ranges from 3°C to 63°C.

2. Geologic Settings

[5] Exposed basalt is present along the active spreading center for most of the JFR and at the latitude of our sites (Figure 1a). East of the ridge axis, Pleistocene turbidites, which are mainly hemipelagic muds with interbeds of silty to sandy turbdites, fill most of the northern portion of Cascadia Basin, resulting in a relatively flat seafloor with a few places where basalt outcrops at the seafloor [*Zühlsdorff et al.*, 2005; *Underwood et al.*, 2005]. One of these basaltic outcrops is Baby Bare, which overlies 63°C, 3.5 Ma crust [e.g., *Davis et al.*, 1997; *Becker et al.*, 2000]. Baby Bare lies on a north-south tending ridge, roughly parallel to the active spreading center to the west. ODP Leg 168 drilled this ridge at ODP Site 1026 (6.6 km north northeast of Baby Bare) and 2.2 km east of this ridge in a sediment trough (ODP Site 1027) [*Davis et al.*, 1997]. Both ODP sites were drilled and cased into the first basaltic contact. ODP Hole 1026b penetrated 66 m of upper basaltic basement. In contrast, ODP Hole 1027C was sealed in a basaltic sill. Thus, below the cased portion of the borehole the open borehole is exposed to 12 m of mudstone and 26 m of upper basaltic basement. IODP Exp 301 drilled Site 1301 ~ 1 km south southwest of ODP Site 1026 along the same underlying basaltic ridge [*Fisher et al.*, 2005]. Four holes were drilled at this site, two of which penetrated basalt and were cased and two that were used to recover a nearly complete sediment profile. All four cased holes (1026B, 1027C, 1301A, and 1301B) were instrumented with a CORK for hydrologic and biogeochemical studies [*Fisher et al.*, 2005].

[6] Two other boreholes were instrumented with a CORK during ODP Leg 168 [*Davis et al.*, 1997] (Figure 1a). One CORK was placed at ODP Site 1024. This site drilled into 0.97 Ma crust with a sediment-basalt contact temperature of ~23°C. The other CORK was deployed at ODP Site 1025, which penetrated 1.24 Ma crust with a sediment-basalt contact temperature of 40.5°C [*Becker and Davis*, 2003]. Both sites penetrated upper basaltic basement, providing an open hole to this formation. These sites are about 26 and 36 km, respectively, east of the active portion of the ridge where young basalt is exposed. The surface of exposed basalt extends from the ridge to ~19 km toward the east, providing a possible source for seawater penetration into the basaltic crust only 7 km from ODP Site 1024. Transport of seawater from this exposed outcrop to the first buried ridge, located about 4 km east of Site 1025, has been postulated [*Elderfield et al.*, 1999; *Davis et al.*, 1999]; however, a component of along axis flow (north-south) is probable [e.g., *Wheat et al.*, 2000; *Fisher et al.*, 2003; *Hutnak et al.*, 2006].

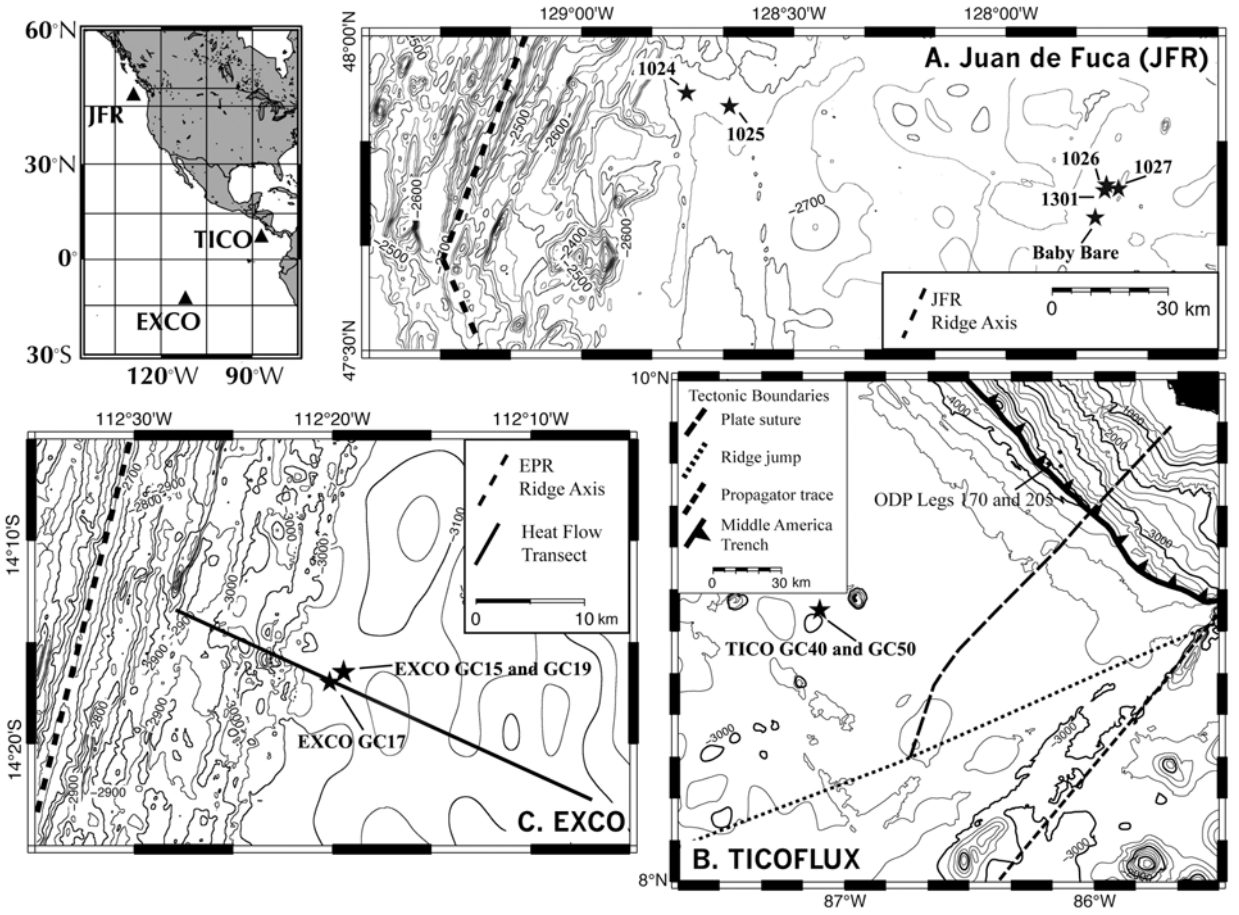

Figure 1. Location of ridge flank hydrothermal systems (RFHS) on the eastern flank of the Juan de Fuca Ridge (JFR), the TicoFlux site, and the EXCO site. (a) Stars represent sites where data are reported, including borehole observatories (CORKs) that were deployed during ODP Leg 168 (Sites 1024–1027 [*Davis et al.*, 1997]) and IODP Exp 301 (Site 1301 [*Fisher et al.*, 2005]), and Baby Bare, a basaltic outcrop with hydrothermal springs [e.g., *Wheat and McManus*, 2005]. Grizzly Bare (not shown; 47°17′N and 128°4′W) is the primary source for basaltic formation fluids at Baby Bare and Sites 1026, 1027, and 1301. (b) Gravity cores 40 and 50 (9°5.05′N and 87°5.93′W) were collected from Dorado Outcrop, a small knoll on the eastern flank of the East Pacific Rise (EPR) west of Costa Rica. Seismic data and short cores that recovered basalt imply that this knoll is a basaltic outcrop similar in size to Baby Bare. (c) Gravity cores 15 (14°16.55′S and 122°19.43′W), 17 (14°16.88′S and 112°19.86), and 19 (14°16.54′S and 122°19.43′W) were collected on the eastern flank of the EPR overlying young crust. Cores were collected from a topographic high that trends in a north-south direction parallel to the active spreading ridge to the west and were positioned relative to a seismic-heat flow transect [*Villinger et al.*, 2002]. Bathymetric data are from the Marine Geoscience Data System (MGDS).

[7] A second RFHS was sampled during the TicoFlux II expedition (20 to 25 Ma crust) on the eastern flank of the Cocos Plate immediately west of the Middle-America Trench (Figure 1b). Sediment pore water Ge concentrations from two gravity cores have been reported [*Wheat and McManus*, 2005]. We report new sediment pore water Ge data from a different site where two gravity cores (GC 40 and 50) were taken from a small basaltic outcrop, Dorado. Measured thermal gradients in the sediment surrounding the Dorado outcrop are low, with heat flow values of 20–30 mW/m^2 [*Hutnak et al.*, 2007]. Yet, on the outcrop the heat flow is at least 1000 mW/m^2 [*Hutnak et al.*, 2007], consistent with the interpretation that basaltic formation fluids vent from this small outcrop in a similar manner to that found on Baby Bare. Coring operations and the presence of basalt fragments at the base of some short (<1 m long) cores are consistent with a thin, but patchy sediment cover with places where basalt is likely exposed.

Table 1. Summary for Dissolved Ge Analyses

Date	Ge Std., pM	Meas., pM	Known/Meas.
Mar '05	110	131 ± 5 (5)	0.84
	Monitor	88 ± 8 (2)	
Jan '06-1[a]	219	231 ± 5 (9)	0.95
	110	109 (1)	1.01
	2755	2760 ± 1 (2)	1.00
Jan '06-2	219	233 ± 5 (5)	0.94
	110	115 (1)	0.96
Jan '06-3[b]	219	214.0 ± 0.3 (2)	1.02
	110	111 (1)	0.99
June '06-1[b]	219	218 ± 5 (4)	1.00
	689	641 (1)	1.07
	2755	2510 (1)	1.10
	Monitor	104 ± 3 (3)	
June '06-2	219	230 ± 10 (4)	0.95
	2755	2640 ± 30 (3)	1.04
	Monitor	99 ± 1 (3)	
June '06-3	219	230 ± 20 (3)	0.95
	2755	2640 (1)	1.04
	Monitor	101 ± 1 (3)	
June '06-4	219	232 ± 8 (7)	0.94
	689	720 ± 50 (3)	0.96
	2755	2480 ± 20 (2)	1.11
	Monitor	58 ± 2 (3)	
Oct '06-1[c]	219	220 ± 10 (4)	0.98
	2755	2700 ± 100 (2)	1.02
Oct '06-2[c]	219	240 ± 5 (3)	0.91
	2755	2600 ± 300 (2)	1.06

[a] Read Jan '06-1 as January 2006, run 1.
[b] Indicates that there were no samples used from these particular runs for this paper. However, we include these values as an added measure of our technique sensitivity.
[c] These standards were used during analysis of sediment solid phases.

[8] The third RFHS is located on 0.3 Ma crust east of the EPR at 14°S (Figure 1c). There are no major fracture zones nearby and spreading is continuous with no major offsets [*Grevemeyer et al.*, 2002]. Measured heat flow is only ~25% of the predicted value, implying that much of the heat is lost from ridge flank hydrothermal circulation [*Villinger et al.*, 2002]. Sediment was cored from a basaltic ridge lying parallel and to the east of the spreading center. Basalt was recovered at the base of several sediment cores at depths as shallow as 3 m, implying a thin sediment cover.

3. Analytical Methods

[9] Sediment pore waters were recovered on ODP Leg 168 by squeezing sediment at room temperature and filtering the fluid through 0.45 μm filters [*Davis et al.*, 1997]. Sediment pore waters collected on IODP Exp 301 were extracted at room temperature within a nitrogen atmosphere and filtered through 0.45 μm filters [*Fisher et al.*, 2005]. Last, sediment pore waters from gravity cores were extracted by centrifugation at 1–4°C and filtered through 0.45 μm filters. These pore water extraction techniques may have introduced sampling artifacts that have influenced our results [e.g., *de Lange et al.*, 1992]. Basaltic formation fluids were collected with continuous fluid samplers (OsmoSamplers) within the open boreholes at ODP Sites 1024 and 1027 [*Wheat et al.*, 2003b] and directly from the venting (producing) boreholes at ODP Sites 1025 and 1026 using Walden-Weiss (Major) titanium syringe samplers [*Wheat et al.*, 2004a]. These syringe samplers were used to collect basaltic formation fluids from springs on Baby Bare [*Wheat and McManus*, 2005].

[10] Inorganic Ge (germanic acid) was measured on pore water samples using an isotope dilution technique [*Mortlock and Froelich*, 1996; *Hammond et al.*, 2000]. Samples are spiked with ^{70}Ge and allowed to equilibrate prior to analysis. Germanic acid is converted to germane (GeH_4), which is then transferred into an ICP-MS for analysis. We typically target a Ge 70:74 ratio of 1 – 10 with the ideal ratio of ~10 [*Mortlock and Froelich*, 1996]; however, this ideal ratio is not always practical [e.g., see *Mortlock and Froelich*, 1996] nor is it always attained because we do not know a priori the Ge concentration for a particular sample. Results can be less precise at high ratios. One reason for this decline in precision is because our ^{74}Ge blanks can become a larger fraction of the total signal, making the calculation of Ge concentrations subject to additional uncertainty. For this reason we have operationally excluded Ge results where the analytical ratio exceeds 25.

[11] We analyzed a series of spiked standards and normalize our results to one of those standards. This normalization is typically small (~5%, Table 1); however, on one occasion (March 2005, Table 1) that correction was ~16%. The most frequently analyzed standard had a concentration of 219 pM Ge. Our analysis of this standard resulted in a calculated average of 230 ± 10 pM (n = 41), excluding one datum more than 4σ from the mean value. On the basis of a variety of standards, the average precision for the data set is better than 5% (Table 1). Standards are typically within 10% of the expected value with the lone exception being analyses conducted on June '06–4 (Table 1). We also measured a seawater sample as a precision monitor (Table 1). The within-run precision of this sample is typically better than 10%. On

Table 2. Standard Reference Material Analyses For Solid Sediments

Standard[a]	Al, %	Ca, %	Fe, %	Mg, %	Mn, ppm	Si, %	Ti, %
USGS BCR (1)	7.13	5.01	9.29	2.08	1440	19.7	1.36
Reported	7.22	5.09	9.39	2.1	1390	16.7	1.34
SX12280 (7)[b]	6.2 ± 0.1	0.90 ± 0.02	3.89 ± 0.07	1.79 ± 0.03	2500 ± 40	23.5 ± 0.8	0.33 ± 0.01
Reported	6.2	1.05	4.18	1.83	2600	26	0.38
NIST 1646A (3)	2.4 ± 0.8	0.31 ± 0.01	2.0 ± 0.7	0.42 ± 0.01	220 ± 7	35 ± 2	0.48 ± 0.01
Reported	2.3	0.52	2.01	0.39	234	40	0.456

[a] Numbers in parentheses represent the number of analyses for each standard. Values for Ge are as follows: BCR Ge = 0.68 ppm, SX12280 Ge = 0.31 ± 0.01 (n = 2), and 1646A Ge = 0.37.
[b] SX12280 is a siliceous clay from MANOP Site S (11°00′N, 140°05′W), and the reported results are from *Robbins et al.* [1984].

the basis of these combined results (summarized in Table 1), we estimate that on average our precision and accuracy are better than 10%, but we note that values outside of this range are occasionally observed. We also reanalyzed three samples reported previously [*Wheat and McManus*, 2005]. Average values from the two analyses for these three samples (samples 2972-13, 2972-11, 2974-13) are consistent with our precision and accuracy expectations (9.4 ± 0.8 nM, 9.6 ± 0.2 nM, and 10.5 ± 0.2 nM, respectively). We previously reported our uncertainty based on the reproducibility of a set of low concentration standards [*Wheat and McManus*, 2005]; however, that uncertainty is inappropriate for high Ge concentration samples. We suggest that the uncertainty in those values is more accurately represented by our assessment in this communication. Dissolved Si was measured in diluted samples using standard ICP-OES techniques with a precision of 3%; all data are either presented in the auxiliary material[1] (Tables S1–S5) or are presented elsewhere [*Davis et al.*, 1997; *Fisher et al.*, 2005; *Wheat et al.*, 2003b, 2004a; *Hulme et al.*, 2008].

[12] A considerably larger concern than analytical variability, particularly for our sediment pore water analyses, is the possibility of sampling artifacts [e.g., *de Lange et al.*, 1992]. Some sediment pore water samples were cooled from in situ temperatures of 63°C to room temperature during handling procedures. Other sediment pore water samples were exposed to the atmosphere, allowing the possibility for Fe oxides or other phases to precipitate during sample handling. Nevertheless, there appears to be no significant Si artifact and concentrations of Fe and Mn are generally a small percentage of Fe and Mn concentrations in continental sediment pore waters where Ge removal has been documented, perhaps as an iron-rich smectite [e.g., *King et al.*, 2000; *Hammond et al.*, 2000; *McManus et al.*, 2003].

[13] Sediment samples were digested using a "fusion" technique [e.g., *Murray et al.*, 2000]. This technique uses ~800 mg of Li metaborate and ~200 mg of sample. Samples are fused at 1100°C for 15 to 20 min and then dissolved in 2 N HNO_3. During analyses every ~8 samples were typically bracketed by a quality control (QC) standard and a standard reference material (USGS BCR1, NIST 1646A, and an in-house standard reference material SX12280, Table 2). Agreement between the reported values and those measured here are generally acceptable; however, the Ca and Si data and one Ti measurement are not. All of the other values match within 10% or better. The analytical (instrument) precision is based on repeat analyses of a SX12280 digest solution (Table 2). Germanium in these samples was also measured by ID-ICPMS. Precision of those analyses is based on repeat analyses of an individual sample as well as analyses of repeat digests of the same sample. Values that are averages of redigested samples are noted in the Table S5 with an asterisk (*). Although some of the uncertainties in these values are larger than we would like, we note that our conclusions are sufficiently robust as to be largely insensitive to these uncertainties. Assuming that our uncertainties are generated randomly, we consider the uncertainty in the pooled Ge:Si ratio to represent the uncertainty in the average Ge:Si ratio. The average Ge:Si molar ratio for the entire data set is 1.0 ± 0.2 (see auxiliary material).

4. Results

[14] We present three different data types: sediment pore water, basaltic formation fluids, and bulk sediment composition. Concentrations of Ge in

[1] Auxiliary materials are available in the HTML. doi:10.1029/2007GC001892.

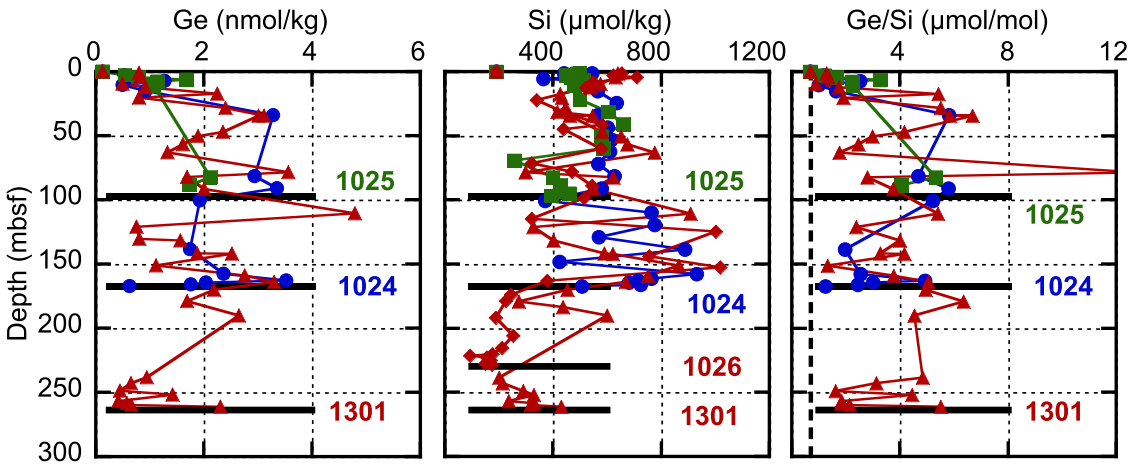

Figure 2. Depth profiles of Ge and Si concentrations and the Ge:Si molar ratios of pore waters from ODP Sites 1024 (blue circles), 1025 (green squares), and 1026 and IODP Site 1301 (red triangles). These sites represent a range of temperatures at the sediment-basement contact (23, 40.5, 63, and 63°C, respectively; Table 3). The calculated Ge:Si molar ratio of sediment pore waters is greater than that of amorphous silica (dashed vertical line) and generally less than 7 μmol/mol. Black horizontal lines represent the depth of basaltic basement. Bottom seawater concentrations are shown (180 μmol Si/kg and 130 pmol/kg; Table 3) [*Wheat and McManus*, 2005].

sediment pore waters from each of the three deep-drilling sediment profiles (ODP Sites 1024 and 1025 and IODP Site 1301) show an increase in concentration from seawater values to ~0.5 nmol/kg in the first sample at a depth of 1.2 to 1.5 meters below seafloor (mbsf) (Figure 2). Concentrations generally continue to increase with depth to ~50 mbsf. Below this depth, concentrations remain relatively uniform at 2 nmol/kg, and decrease with depth in the lower 50 m of the sediment. These trends are similar to those of Si, except concentrations of Si are relatively uniform in the upper 50 m of the sediment. The average sediment pore water Ge:Si molar ratio is ~4 μmol/mol, which is higher than the ratio in bulk sediment (1.0 ± 0.2 μmol/mol).

[15] Concentration-depth profiles of Ge in sediment pore waters from the two gravity coring operations are distinct. The two sediment pore water profiles from the TicoFlux site show increasing concentrations of Ge and Si with depth, reaching asymptotic concentrations. These sediment pore waters have an average Ge:Si molar ratio of 2 μmol/mol (Figure 3). In contrast, the three sediment pore water profiles from the EXCO site have Ge concentrations that decrease with depth below the bottom seawater concentration, then increase to a concentration that is close to the bottom seawater value at the base of the core (Figure 3). The Si data for these sediment pore waters show an increase in concentration with depth followed by a decrease in concentration with depth as the sediment-basalt interface is approached. Shapes of these Si profiles are consistent with the upward flow of basaltic formation fluids through the sediment [e.g., *Wheat and Tribble*, 1994; *Wheat and McDuff*, 1994]. Phosphate and nitrate (not shown) data confirm the presence of active hydrothermal seepage through the sediment section [e.g., *Wheat and McDuff*, 1994]. The calculated Ge:Si molar ratio of these sediment pore waters is ~0.4 μmol/mol, which is lower than the Ge:Si molar ratio in present-day diatoms (0.7 μmol/mol [*Shemesh et al.*, 1989]).

[16] Concentrations of Ge in basaltic formation fluids were obtained from four ODP boreholes and Baby Bare springs (Table 3). Although Si concentrations in borehole fluids and spring fluids fall within the range measured in basal sediment pore waters immediately above these boreholes, concentrations of Ge are considerably higher in borehole fluids relative to basal sediment pore waters with the exception of data from ODP Site 1024. All four of these borehole sites have a Ge:Si molar ratio that is at least twenty times greater than that of seawater.

[17] Chemical analyses of bulk sediment from IODP Site 1301 result in an average Ge concentration of 0.65 ppm, excluding the one low sample (Figure 4). This sample with an exceptionally low Ge concentration also is depleted in Si, Al, Ti, Fe, and Mg and enriched in Mn and Ca. This sample

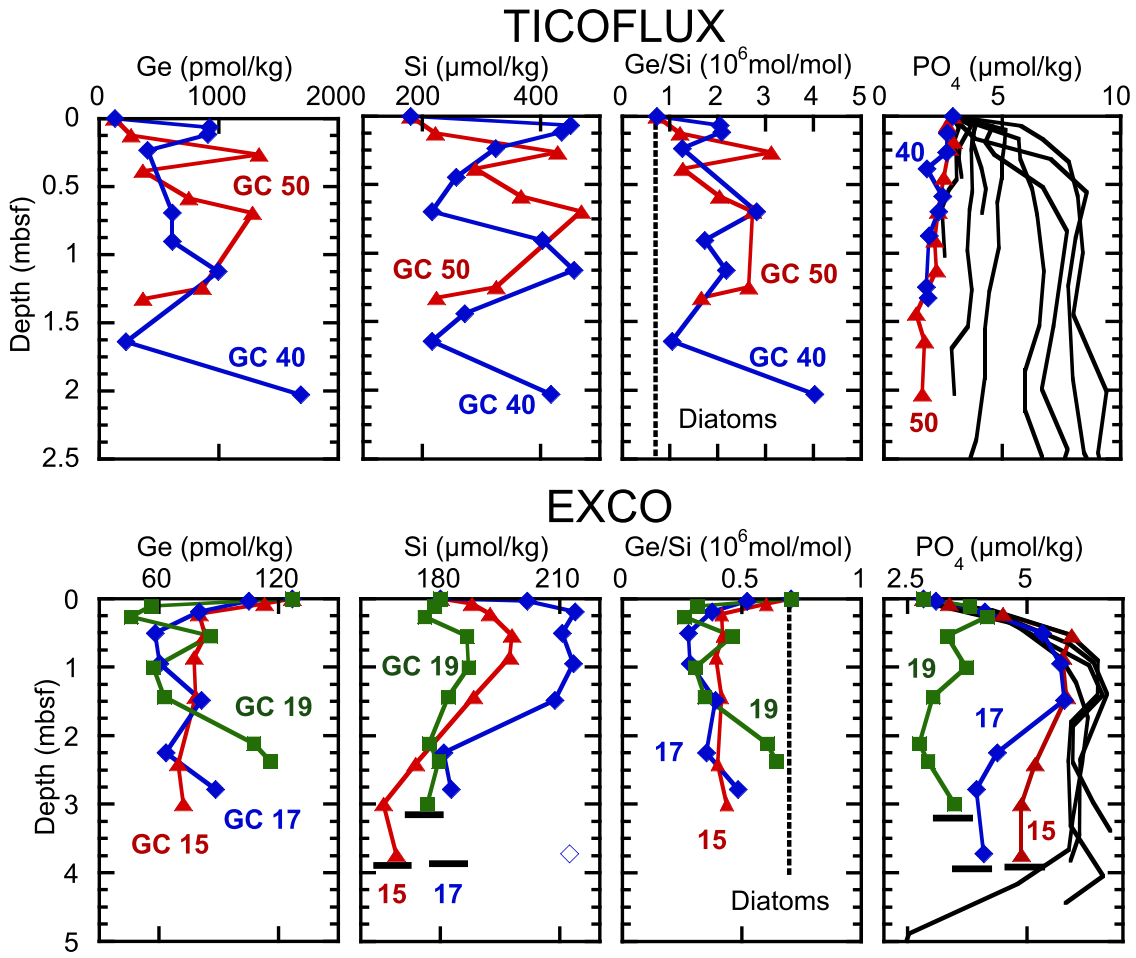

Figure 3. Depth profiles of Ge, Si, and PO_4 concentrations and the Ge:Si molar ratio from TicoFlux and EXCO sites. Sediment pore water data from the TicoFlux cores (GC 50, red triangles; GC 40, blue diamonds) are similar to those from the JFR. In contrast, sediment pore water Ge concentrations are less than expected bottom seawater values at the EXCO site, resulting in Ge:Si molar ratios that are less than the present-day ratio in diatoms (dashed vertical line) (GC 15, red triangles; GC 17, blue diamonds; GC 19, green squares). Phosphate data are presented to illustrate the presence of upward seepage of basaltic formation fluids through the sediment section [e.g., *Wheat et al.*, 1996]. Phosphate profiles represented by black lines have much slower or no hydrothermally driven flow. Black horizontal lines represent the depth to basalt, based on the presence of basaltic fragments or dented core cutters. Bottom seawater values are from the TicoFlux expedition.

has a Ge:Si molar ratio that is indistinguishable from the average sediment value.

5. Discussion

[18] In general, ridge flank hydrothermal circulation is restricted to the permeable upper basaltic crust [e.g., *Fisher et al.*, 2003; *Hutnak et al.*, 2006] with minimal seepage through overlying sediment [e.g., *Spinelli et al.*, 2004] (Figure 5). As bottom seawater enters basaltic crust, through faults and outcrops, it warms and reacts with basalt, resulting in a basaltic formation fluid composition that differs from that of bottom seawater. The composition of the basaltic formation fluid also is affected by diffusive exchange with overlying sediment pore water. Where sediment cover is thin, it is possible for basaltic formation fluids to seep from the crust (e.g., TicoFlux and EXCO sites) and even form springs (e.g., Baby Bare). However, where sediment thickness is too great (e.g., Sites 1024, 1025, and 1301), no advective transport of basaltic formation fluids through the sediment is possible [e.g., *Wheat and Mottl*, 1994].

[19] Basaltic formation fluids from the 3.5 Ma crust on the eastern flank of the JFR are fed from seawater that enters basalt through Grizzly Bare, located ~52 km to the SSW of Baby Bare [*Wheat*

Table 3. Measured and Estimated Values for Basaltic Formation Fluids

Sites[a]	Ge, nmol/kg	Si, mmol/kg	Ge/Si, μmol/mol	Temp., °C	Mg, mmol/kg
Seawater (1)	0.13	0.18	0.72	2	52.5
Cold RFHS					
TicoFlux	0.30	0.18	1.67	7	52
EXCO	0.12	0.17	0.73	3	52.5
Cool RFHS					
1024 (2)	0.75	0.05	17	23	43.1
Warm RFHS					
1025 (3)	8.7	0.58	15	40.5	27.7
1026 (3)	19	0.71	27	63	2
1027 (2)	20	0.32	62	63	1
Baby Bare (1)	11.3	0.36	34	63	1

[a] Estimates and data not presented in the auxiliary material are from 1, *Wheat and McManus* [2005]; 2, *Wheat et al.* [2003b]; and 3, *Wheat et al.* [2004a].

et al., 2000; *Fisher et al.*, 2003; *Hutnak et al.*, 2006] (Figure 5). The net result of reaction and diffusive exchange is an increase in the concentrations of Ge and Si and an increase in the Ge:Si molar ratio of spring fluid at Baby Bare [*Wheat and McManus*, 2005]. Because the Ge:Si molar ratio of these fluids is much higher than that of source materials, *Wheat and McManus* [2005] concluded that preferential removal of Si from the basaltic formation fluid relative to Ge must occur, requiring extensive dissolution/precipitation reactions (e.g., Rayleigh distillation [*Evans and Derry*, 2002]). On the basis of this initial data, we collected additional data to address two questions: (1) do these reactions occur in basal sediments or within the basaltic crust, and (2) does the temperature of upper basaltic crust affect Ge concentrations in RFHS?

[20] To address these questions we group the data according to the temperature in upper basaltic basement. Data from warm (~30 to 70°C) RFHS are presented first, because they provide distinct evidence for the lack of a sediment control on Ge

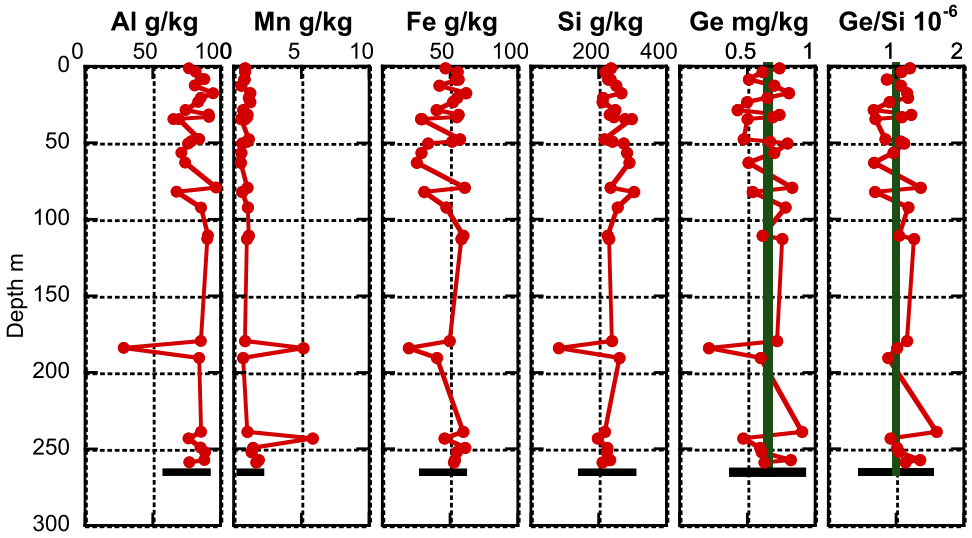

Figure 4. Bulk chemical analysis of sediment from IODP Site 1301 plotted as a function of depth. Ti, Ca, and Mg data are not shown. Ti and Mg data match Al and Fe data. Ca data match Mn data. These data are consistent with those from ODP Sites 1026 and 1027 [*Buatier et al.*, 2001]. Note the one sample with anomalously low concentrations of Al, Ti, Fe, Mg, Si, and Ge. This hydrothermally altered sample has anomalously high concentrations of Mn and Ca, but the low concentrations of Ge indicate that Ge is not sequestered into either carbonate- or Mn-oxide-rich minerals. Green vertical lines in the Ge and Ge:Si plots are average values for the entire sediment column, excluding the one sample with a low Ge concentration.

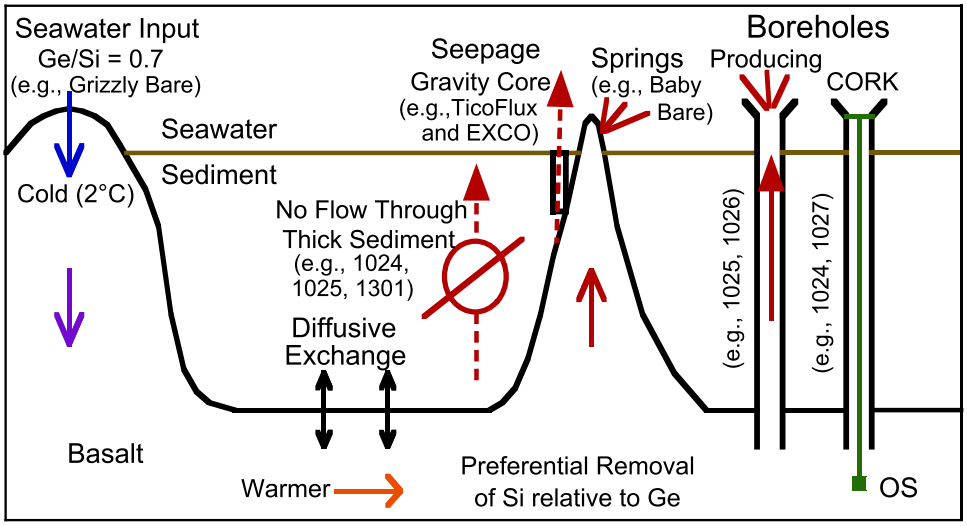

Figure 5. Cartoon of seawater flow though a ridge flank hydrothermal system. Seawater enters a basaltic outcrop and warms. This fluid is altered by diffusive exchange with the overlying sediment and reactions within the basaltic crust. We show four means one can use to sample basaltic formation fluid: gravity cores in areas with thin sediment cover and focused upward seepage of basaltic formation fluids (e.g., TicoFlux and EXCO), springs (e.g., Baby Bare), producing boreholes (e.g., ODP Sites 1025 and 1026), and continuous fluid samplers (OsmoSamplers, OS) that are deployed within "CORKed" boreholes (e.g., ODP Sites 1024 and 1027). Sediment, which is less permeable than the upper basaltic crust, restricts hydrothermal flow of basaltic formation fluids to seawater. If the sediment is sufficiently thick (e.g., ODP Sites 1024 and 1025 and IODP Site 1301), hydrothermal flow through the sediment is not possible under natural conditions.

cycling. These data were collected from ODP Site 1025 and along a transect defined by Grizzly Bare-Baby Bare-IODP Site 1301-ODP Site 1026-ODP Site 1027. Cold (3–10°C) RFHS are presented second, because Ge cycling is largely impacted by sedimentary processes. Here we present sediment pore water data from TicoFlux and EXCO. At these sites bottom seawater enters the basaltic crust from outcrops or faults with exposed basalt and is altered along its flow path before venting from the crust. The length of this flow path is likely tens of kilometers, which is the distance to the nearest outcrop for the TicoFlux site and to the active spreading center to the west of the EXCO site. More data are needed to refine these distances. Last, both basaltic and sedimentary process affect Ge cycling in cool (20–30°C) RFHS (e.g., ODP Site 1024).

5.1. Warm (~30 to 70°C) Ridge Flank Hydrothermal Systems

[21] There is a range in Ge concentrations for borehole fluids from ODP Sites 1026 and 1027 and spring fluids from Baby Bare, even though the crustal temperature is estimated to be the same and all three sites are located within 8 km of each other (Figure 1 and Table 3). Fluid from Baby Bare springs represents the most pristine basaltic formation fluid. This assumption is consistent with a single linear mixing trend between Ge and Mg in spring (basaltic formation) fluids and bottom seawater [*Wheat and McManus*, 2005]. Similarly, Si data show a single trend with Mg, in contrast to some other elements that are more reactive in the sediment column (e.g., Mn, Co, Ni, Cd, Zn, and Mo [*Wheat et al.*, 2002]). Given this single linear trend, Ge and Si in Baby Bare fluids are not overprinted by diagenetic processes. In contrast, borehole fluid compositions from ODP Sites 1026 and 1027 appear to have a sedimentary component that affects the concentration of Si and other ion concentrations [e.g., *Wheat et al.*, 2003b, 2004a]. The Ge concentration in basaltic formation fluids from both of these boreholes is considerably greater than that from Baby Bare. We believe that this range in Ge concentrations and Ge:Si molar ratios results from reaction with sediment at the base of these boreholes [*Wheat et al.*, 2003b, 2004a]. Alternatively, the range in observations could result from the path of fluid circulation within the crust. Basaltic formation fluid flows north past Baby Bare before reaching ODP Sites 1026 and 1027. This path and the Ge data would imply that if the residence time (kinetic constraints) within the basaltic crust is a dominate factor, then fluids with

long residence times should have higher concentrations of Ge. This explanation is not supported by the ^{14}C data [*Elderfield et al.*, 1999], provided that the calculated ^{14}C age is a good relative proxy for the actual fluid age. For example, the oldest ^{14}C aged fluid from these sites is found at ODP Site 1024, but these fluids do not have the highest Ge concentration.

[22] What is the source for these high Ge concentrations and Ge:Si molar ratios in basaltic formation fluids? The source is either the sediment, the basalt, or a combination of both. The sediment pore water data provide clear evidence that the sediment is not the source for these high values in basaltic formation fluids. We thought Ge would be sequestered during the early sediment depositional history [e.g., *King et al.*, 2000; *Hammond et al.*, 2000, 2004; *McManus et al.*, 2003]. With time as the crust warms and hydrothermal circulation develops, basal Fe- or Mn-rich or metalliferous sediments undergo Mn and Fe reduction [*Buatier et al.*, 2001; *Fisher et al.*, 2005], liberating dissolved Fe, Mn, and presumably Ge to the sediment pore water that then diffuses into basaltic formation fluids. However, sediment pore water from ODP Site 1301 have Ge concentrations that are ~2 nmol/kg, much less than the concentration found in spring fluids from Baby Bare (11.3 nmol/kg) (Table 3). Provided these sediment pore water data are broadly representative, high Ge concentrations in basaltic formation fluids are controlled by reactions within basaltic crust.

[23] The same conclusion is reached with data from ODP Site 1025 (40.5°C) (Figure 3 and Table 3). At this site the average basal sediment pore water Ge concentration is ~2 nmol/kg with a Ge:Si molar ratio of ~4 μmol/mol. These values are much lower than those measured in basaltic formation fluids that vent from the borehole (8.7 nmol/kg and 15 μmol/mol, respectively). These findings indicate that there is a broad crustal temperature range over which reactions within basalt dominate Ge and Si cycling.

[24] Chemical analysis of bulk sediment from IODP Site 1301 was undertaken to determine if diagenetic reactions or the influence from diffusive exchange from basaltic formation fluids have an observable affect on sediment concentrations. Our data, which are consistent with those published for ODP Site 1026 [*Buatier et al.*, 2001], show relatively uniform downcore sedimentary Ge concentrations and Ge:Si molar ratios. The average sedimentary Ge:Si molar ratio is 1.0 ± 0.2 μmol/mol, which is about that of present-day diatoms, but much less than the sediment pore water value. Therefore, preferential removal of pore water Si relative to Ge must occur within the sediment. One interesting feature of our sediment data is the one sample with anomalously low Al, Ti, Fe, Mg, Si, and Ge concentrations. This sample also has anomalously high concentrations of Mn and Ca, consistent with a hydrothermal source [e.g., *Buatier et al.*, 2001, 2004]. Oddly, this sample has a low sedimentary Ge concentration with a Ge:Si molar ratio of 1.0 μmol/mol, suggesting Ge is not preferentially removed in manganese oxides or carbonates.

[25] Unlike the case for other sediment reactive elements in basal sediments from nearby boreholes (e.g., Mn and Fe [*Buatier et al.*, 2001, 2004]), there is no observable increase in the basal sedimentary Ge concentration. This observation is consistent with estimates for the diffusive flux of Ge from basaltic formation fluids to overlying sedimentary pore waters. If the diffusive flux is [*Berner*, 1980]

$$\mathrm{Flux}_{\mathrm{diffusion}} = \emptyset(D_0/(\mathrm{FF}))\Delta C/\Delta z, \quad (1)$$

where ø is the sediment porosity (0.55 [*Wheat et al.*, 2000]), D_0 is a diffusion coefficient at infinite dilution extrapolated for Ge at 63°C [*Li and Gregory*, 1974], FF is the formation factor (6 [*Wheat et al.*, 2000]), and $\Delta C/\Delta z$ is the Ge concentration gradient defined by the deepest sediment pore water concentration at IODP Site 1301, a basaltic formation fluid concentration (11.3 nmol/kg; Baby Bare), and a length of 3.9 m, then the calculated flux is 1.6 pmol Ge/cm^2/a. Given the sedimentation rate and the sediment thickness required to impede flow through the sediment and warm the crust [*Underwood et al.*, 2005; *Wheat and Mottl*, 1994], such chemical gradients probably have persisted for the past 220 ka [*Wheat et al.*, 2004b], resulting in a net flux of 360 nmol Ge/cm^2. If this flux is deposited uniformly over the basal 3 m of the sediment, which represents the deepest sediment sample, only a 4% increase is expected. This change would not be observed given our analytical capabilities.

5.2. Cold (3–10°C) Ridge Flank Hydrothermal Systems

[26] Sediment pore water data from the TicoFlux site are similar to those from the JFR in that concentrations of Ge and Si and the Ge:Si molar ratio are well above seawater values. Although heat flow data and systematic variations in sediment pore water profiles of phosphate and alkalinity (not

shown) are consistent with vertical upward seepage through these cores (Figure 3) [e.g., *Wheat et al.*, 1996], flow is sufficiently slow that diagenetic reactions involving Ge and Si mask typical advection-diffusion profiles. Similar to the ODP and IODP profiles, these profiles are not as "smooth" as those from coastal settings. We suspect that these results are influenced by a variety of sediment types and ages that were cored; however, as discussed above methodological artifacts cannot be discounted as possible influences on our data. Even though the TicoFlux cores are <3m in length, they were collected from the slopes of a seamount, consisting of a variety of sediment types, representing a compressed history of sedimentation on this ~20 Ma-old feature [e.g., *Spinelli and Underwood*, 2004].

[27] Data from the EXCO site show systematic trends in sediment pore water Ge and Si concentrations. Calculated sediment pore water upwelling speeds range from ~0.1 to 10 cm/a, on the basis of an advection-diffusion-reaction model for Si with a basaltic formation fluid that has a concentration ~20 μmol/kg less than that of bottom seawater [e.g., *Wheat and Tribble*, 1994; *Wheat and McDuff*, 1994]. As this low Si, sediment pore water ascends it reacts with sediment and dissolves amorphous silica, resulting in a measurable change in dissolved Si concentrations. Similarly, we expect a corresponding and proportional increase in the Ge concentration [e.g., *King et al.*, 2000] of ~23 pmol/kg for GC 17 (Figure 3). Yet, concentrations of Ge in sediment pore waters from this core are less than the seawater concentration and the estimated concentration of 120 pmol/kg for the basaltic formation fluid, which is based on the concentration measured in the deepest sample from cores that recovered pieces of basalt. Therefore, Ge is preferentially removed relative to Si from the upwelling pore water into secondary minerals. Sequestration of Ge by sediments has been documented in shallow sediment where reduced dissolved Fe is oxidized [e.g., *King et al.*, 2000; *Hammond et al.*, 2000; *McManus et al.*, 2003]. However, in this setting, nitrate concentrations increase as the fluid ascends while Mn and Fe concentrations generally remain below detection (0.05 umol/kg) [e.g., *Bender et al.*, 1985/1986; *Wheat and McDuff*, 1994]. Given the lack of diagenetic Fe-oxides and sulfides in this environment, Ge is likely removed during the formation of secondary clays [e.g., *Kurtz et al.*, 2002; *Scribner et al.*, 2006].

[28] Sediment pore water data from the TicoFlux and EXCO sites are quite different, thereby making a straightforward characterization of cold RFHS impossible. These differences may reflect the sediment composition. For example, EXCO sediment has a greater volcanic component. In short, the composition of basaltic formation fluids that ascend the sediment at these sites is similar to, and perhaps, less than the seawater concentration, but significant diagenetic reactions prohibit a definitive conclusion. Therefore, cold RFHS may either be a net source or a net sink of Ge to the oceans, as could Si. Sediment pore water compositions alone are not sufficiently sensitive to make a quantitative prediction. Additional data from "cold springs" are necessary for such a characterization.

5.3. Cool (20–30°C) Ridge Flank Hydrothermal Systems

[29] Data from ODP Site 1024 (23°C) provide a transition between warm RFHS that are dominated by reactions within basaltic crust and cold RFHS that are heavily influenced by diagenetic processes within the overlying sediment. At this site, sediment pore water profiles are similar to those from warm RFHS and data from the TicoFlux site. Note the trend of decreasing Ge in the four basal sediment pore water samples from 3.6 nmol/kg to 0.6 nmol/kg (Figure 2). These samples extrapolate to a Ge concentration of ~0.4 nmol/kg at the sediment-basalt interface. This concentration is similar to the average concentration measured in samples collected from the borehole using an OsmoSampler (~0.75 nmol Ge/kg). In contrast to warm RFHS, there appears to be a sedimentary flux of Ge to basaltic formation fluids. Similar to warm RFHS, reactions within the basaltic crust preferentially remove Si into secondary minerals relative to Ge to achieve a Ge:Si molar ratio of 17 μmol/mol (Table 3). The net result of these reactions is a fluid with a Ge:Si molar ratio that is greater than simple dissolution of known source materials.

6. Reaction Systematics Within Basaltic Crust

[30] Higher concentrations of Ge and Ge:Si molar ratios in basaltic formation fluids compared to those in the overlying sediment pore waters requires a net removal of Ge from the basaltic crust. This conclusion is not necessarily intuitive because veins and alteration halos, which are

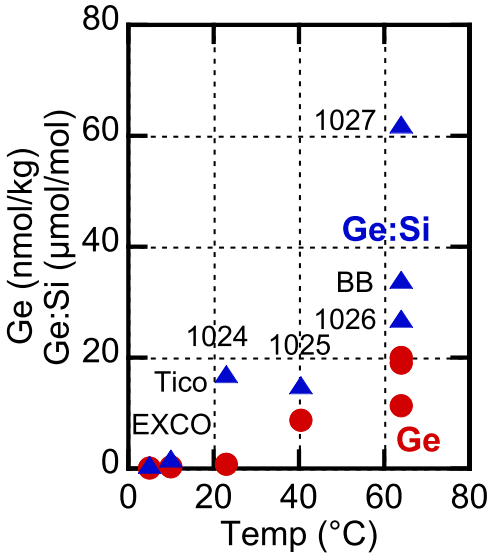

Figure 6. Concentration of Ge (red circles) and the Ge:Si molar ratio (blue diamonds) are plotted versus temperature for upper basaltic basement (Table 3). Labels above or to the left of the blue triangles indicate the site from which the data were collected. The range of values at 63°C may reflect processes associated with the sill at ODP Site 1027, sediment-formation fluid reactions at the base of ODP Site 1026, and longer fluid residence times in basaltic basement following the fluid flow path from Baby Bare to ODP Site 1026 to ODP Site 1027.

ubiquitous within basaltic crust [e.g., *Alt*, 2004], provide a mechanism for the removal of Ge into secondary sulfides, basal iron-rich (metalliferous) sediment, silicate clays, Fe and Mn oxides, and secondary quartz [*Fryklund and Fletcher*, 1956; *Bischoff et al.*, 1983; *Arnorsson*, 1984; *Bernstein*, 1985; *Kolodny and Halicz*, 1988; *Mortlock et al.*, 1993; *Evans and Derry*, 2002; *Kurtz et al.*, 2002]. Our combined data set also implies that Si is removed preferentially relative to Ge in the basaltic crust. Earlier we postulated that the precipitation of secondary quartz, which has a Ge:Si molar ratio of 0.5 μmol/mol [*Mortlock et al.*, 1993; *Kurtz et al.*, 2002], is a likely product [*Wheat and McManus*, 2005].

[31] Here, we present two additional possible processes that may influence the crustal Ge cycle. The first process stems from a plot that shows an increase in Ge and Ge:Si values in basaltic formation fluids with increasing temperature (Table 3 and Figure 6). Inverse trends are observed in plots of Ge and Ge:Si versus Mg, which is not surprising given the observed Mg versus temperature trend [e.g., *Mottl and Wheat*, 1994; *Elderfield et al.*, 1999].

[32] We suspect Ge and Mg concentrations in basaltic formation fluids are linked. In Figure 7 we plot the concentration anomaly, calculated as the difference in the concentrations of basaltic formation fluids and bottom seawater for Mg and Ge. The Mg and Ge anomalies are small at temperatures <25°C. These anomalies increase with increasing temperature, with a maximum possible Mg anomaly resulting from the complete removal of Mg in basaltic formation fluids (e.g., the concentration in bottom seawater; 52.5 mmol/kg). Mg is removed from seawater primarily into smectites that fill voids within the basalt. We suspect that Mg concentrations in basaltic formation fluids reach an "equilibrium" or steady state concentration that is a function of temperature. The depletion of Mg relative to seawater requires more than twice as much Si be removed from the basaltic formation fluid if Mg is removed in the mineral saponite (e.g., $Ca_{0.25}(Mg,Fe)_3(Si,Al)_4O_{10}(OH)_2{\cdot}nH_2O$) [*Schramm et al.*, 2005]. If celadonite is the primary Mg sink, even more Si must be removed given a Mg:Si molar ratio of ~8 for celadonite [*Schramm*

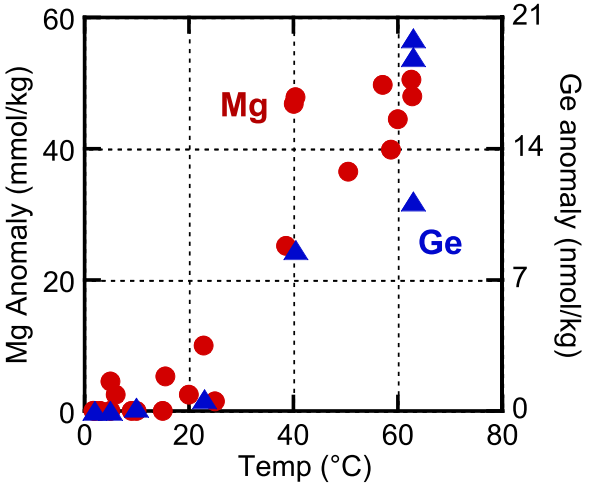

Figure 7. Mg (red circles) and Ge (blue triangles) concentration anomalies in basaltic formation fluids relative to bottom seawater are plotted versus temperature at the sediment-basaltic basement contact. Trends for both elements match one another with minimal anomalies at low temperatures (<25°C). The Mg anomaly is limited by the concentration in bottom seawater; thus by definition the Mg anomaly plateaus at 52 mmol/kg. In contrast, the Ge anomaly is limited by the solubility of secondary minerals, a value that we do not know at this point. Mg data are from *Mottl and Wheat* [1994] and *Elderfield et al.* [1999].

et al., 2005]. In addition to a seawater source of Mg to the basaltic crust, Mg also is leached from primary basaltic minerals. This basaltic source of Mg to the basaltic formation fluid must precipitate as secondary minerals because Mg concentrations in basaltic formation fluids in warm RFHS are less than seawater values [e.g., *Alt*, 2004]. Similarly, Si in basaltic formation fluids has several potential sources: dissolution of basaltic minerals, diffusive exchange with the overlying sediment pore waters, and seawater. Si is removed in smectites with Mg and without Mg in quartz veins. This transfer of Si, from primary basaltic minerals to secondary clays, is associated with a corresponding release of Ge to basaltic formation fluids, consistent with Ge concentrations in altered basalt that are less than those in fresh basalt [e.g., *Koga*, 1967; *Arnorsson*, 1984].

[33] The extent of Ge and Si mobilization in basaltic crust appears to be quite large. If we use the Baby Bare springs as an example, a minimum of 50 mmol Mg/kg must be removed from seawater. This does not account for any Mg that is released from primary basaltic minerals. To remove this much Mg in the form of saponite requires 100 mmol Si/kg that must come from primary basaltic minerals. A corresponding release of 260 nmol Ge/kg is expected, given a bulk basaltic ratio of 2.6 μmol Ge/mol Si [*de Argolla and Schilling*, 1978]. Four times more Ge ($\sim$1 μmol/kg) and Si need to be mobilized if celadonite (instead of saponite) is the primary alteration mineral that forms in the basaltic crust. Additional Ge and Si must be mobilized from primary basaltic minerals to account for the presence of quartz veins. Given a Baby Bare spring fluid with a concentration of 11.3 nmol Ge/kg [*Wheat and McManus*, 2005], most (>96%) of the Ge that is released from primary basaltic minerals must be removed as alteration products within the crust: Fe-rich minerals [*Yatabe et al.*, 2000]; basal iron-rich (metalliferous) sediment [*Buatier et al.*, 2001]; secondary sulfides [*Hunter et al.*, 1999; *Marescotti et al.*, 2000]; silicate clays [*Porter et al.*, 2000]; and secondary quartz [*Porter et al.*, 2000].

[34] A second mechanism that can affect the Ge:Si molar ratio of the basaltic formation fluid is the relative stability of aqueous complexes of both elements. Laboratory studies show an increase in the Ge:Si molar ratio of fluids that are in contact with Ge-bearing silicates with temperature [*Pokrovski and Schott*, 1998a]. Ge also forms aqueous complexes with organic matter, in contrast to Si [*Pokrovski and Schott*, 1998b]. Therefore, the increase in temperature and the presence of dissolved organic matter in basaltic formation fluids favor higher Ge:Si molar ratios. However, increased solubility of Ge relative to Si, as a product of aqueous complexes, is unlikely to be the sole mechanism that produces the observed results.

7. Conclusions

[35] The initial Ge data from spring fluids in RFHS required an explanation that includes extensive dissolution and precipitation reactions (e.g., Rayleigh distillation) and a source from either the overlying sediment or basalt. At warm temperatures (>30°C) processes within RFHS produce concentrations of Ge in basaltic formation fluids that are much greater than sediment pore water concentrations. This high value, high Ge:Si molar ratios, and the removal of Mg into secondary smectites argue for extensive release of Si and Ge from primary basaltic minerals and the subsequent removal of most of this Si and Ge in the form of secondary minerals including smectites and quartz. Given the average Ge:Si molar ratio of 4 μmol/mol in sediment pore water, similar exchange processes must occur in the sediment, which is also the recipient of a diffusive flux of Ge from basaltic formation fluids.

[36] "Cool" RFHS, represented by data from ODP Site 1024 (23°C at the sediment-basalt interface), have a basaltic formation fluid with a Ge:Si molar ratio that is much higher than sedimentary or basaltic sources and seawater. The measured Ge concentration gradient in basal sediment pore waters indicates that "cool" sediments are a source of Ge to basaltic formation fluids. However, the Ge:Si molar ratio in basaltic formation fluids requires a significant basaltic component, consistent with a measurable decease in the Mg concentration of the basaltic formation fluid and the requirement that this decrease results from the formation of secondary minerals that incorporate Si.

[37] The fate of Ge within the basaltic crust of "cold" RFHS (<10°C) is not clear, because neither spring nor basaltic formation fluids have been collected directly and sediment pore water samples that have been collected are altered by diagenetic processes as basaltic formation fluids ascend the sediment column. At the TicoFlux site it appears that the crust is a hydrothermal source of Ge to the oceans, where as at the other site, EXCO, sediment pore water data are consistent with the crust being

a hydrothermal sink for Ge. Given the vast amount of seawater that flows through the ocean crust at "cold" temperatures, even a small Ge anomaly could have a substantial impact on the Ge oceanic budget. Basaltic formation fluids must be sampled directly from cold RFHS to clarify this potentially important source or sink for Ge.

Acknowledgments

[38] We thank Kate Howell, Andy Ross, Andy Ungerer, and Bobbi Conard for analytical assistance and J. Gieskes and an anonymous reviewer for thoughtful comments that improved the manuscript. This research used samples and/or data provided by the Integrated Ocean Drilling Program (IODP). Funding for this research was provided by JOI USSSP and NSF grants OCE 04-00462 to C.G.W. and 0327016 and 0326574 to J.M.

References

Alt, J. C. (2004), Alteration of the upper oceanic crust: Mineralogy, chemistry, and processes, in *Hydrolgeology of the Oceanic Lithosphere*, edited by E. E. Davis and H. Elderfield, pp. 495–533, Cambridge Univ. Press, Cambridge, U.K.

Arnorsson, S. (1984), Germanium in Icelandic geothermal systems*Geochim. Cosmochim. Acta*, *48*, 2489–2502.

Becker, K., and E. E. Davis (2003), New evidence for age variation and scale effects of permeabilities of young oceanic crust from borehole thermal and pressure measurements, *Earth Planet. Sci. Lett.*, *210*, 495–508.

Becker, N. C., C. G. Wheat, M. J. Mottl, J. L. Karsten, and E. E. Davis (2000), A geological and geophysical investigation of Baby Bare, locus of a ridge-flank hydrothermal system in the Cascadia Basin, *J. Geophys. Res.*, *105*, 23,557–23,568.

Bender, M. L., A. Hudson, D. W. Graham, R. O. Barnes, M. Leinen, and D. Kahn (1985/1986), Diagenesis and convection reflected in pore water chemistry on the western flank of the East Pacific Rise, 20°S, *Earth Planet. Sci. Lett.*, *76*, 71–83.

Berner, R. A. (1980), *Early Diagenesis*, Princeton Univ. Press, Princeton, N. J.

Bernstein, L. R. (1985), Germanium geochemistry and mineralogy, *Geochim. Cosmochim. Acta*, *49*, 2409–2422.

Bischoff, J. L., R. J. Rosenbauer, P. J. Aruscavage, P. A. Baedecker, and J. G. Crock (1983), Sea-floor massive sulfide deposits from 21°N, East Pacific Rise, Juan de Fuca Ridge, and Galapagos Rift: Bulk chemical composition and economic implications, *Econ. Geol.*, *78*, 1711–1720.

Buatier, M. D., C. Monnin, G. L. Fruh-Green, and A.-M. Karpoff (2001), Fluid-sediment interactions related to hydrothermal circulation in the eastern flank of the Juan de Fuca Ridge, *Chem. Geol.*, *175*, 343–360.

Buatier, M. D., D. Guillaume, C. G. Wheat, L. Hervé, and T. Adatte (2004), Mineralogical characterization and genesis of hydrothermal Mn oxides from the flank of the Juan the Fuca Ridge, *Am. Miner.*, *89*, 1807–1815.

Davis, E. E., , et al. (Eds.) (1997), *Proceedings of the Ocean Drilling Program, Initial Reports*, vol. 168, Ocean Drill. Program, College Station, Tex.

Davis, E. E., D. S. Chapman, K. Wang, H. Villinger, A. T. Fisher, S. W. Robinson, J. Grigel, D. Pribnow, J. Stein, and K. Becker (1999), Regional heat-flow variations across the sediment Juan de Fuca Ridge eastern flank: Constraints on lithospheric cooling and lateral hydrothermal heat transport, *J. Geophys. Res.*, *104*, 17,675–17,688.

de Argolla, R. M., and J.-G. Schilling (1978), Ge/Si and Ga/Al fractionation in volcanic rocks, *Geochim. Cosmochim. Acta*, *42*, 623–630.

de Lange, G. J., R. E. Cranston, D. H. Hydes, and D. Boust (1992), Extraction of pore water from marine sediments: A review of possible artifacts with pertinent examples from the North Atlantic, *Mar. Geol.*, *109*, 53–76.

Elderfield, H., C. G. Wheat, M. J. Mottl, C. Monnin, and B. Spiro (1999), Fluid and geochemical transport through oceanic crust: A transect across the eastern flank of the Juan de Fuca Ridge, *Earth Planet. Sci. Lett.*, *172*, 151–169.

Evans, M. J., and L. A. Derry (2002), Quartz control of high germanium/silicon ratios in geothermal waters, *Geology*, *30*, 1019–1022.

Fisher, A. T., et al. (2003), Hydrothermal recharge and discharge across 50 km guided by seamounts on a young ridge flank, *Nature*, *421*, 618–621.

Fisher, A. T., T. Urabe, A. Klaus, and the Expedition 301 Scientists (2005), Juan de Fuca Hydrogeology, *Proc. Integr. Ocean Drill. Program*, *301*, doi:10.2204/iodp.proc.301.2005.

Froelich, P. N., and M. O. Andreae (1981), The marine geochemistry of germanium: Ekasilicon, *Science*, *213*, 205–207.

Froelich, P. N., G. A. Hambrick, M. O. Andreae, R. A. Mortlock, and J. M. Edmond (1985), The geochemistry of inorganic germanium in natural waters, *J. Geophys. Res.*, *90*, 1133–1141.

Froelich, P. N., V. Blanc, R. A. Mortlock, S. N. Chilrud, W. Dunstan, A. Udomkit, and T. H. Peng (1992), River fluxes of dissolved silica to the ocean were higher during glacials: Ge/Si in diatoms, rivers, and oceans, *Paleoceanography*, *7*, 739–767.

Fryklund, V. C., and J. D. Fletcher (1956), Geochemistry of sphalerite from Star mine, Coeur d'Alene district, Idaho, *Econ. Geol.*, *51*, 223–247.

Grevemeyer, I., B. Schramm, C. W. Devey, D. S. Wilson, B. Jochum, J. Hauschild, K. Aric, H. W. Villinger, and W. Weigel (2002), A multibeam-sonar, magnetic and geochemical flowline survey at 14°14′S on the southern East Pacific Rise: Insights into the fourth dimension of ridge crest segmentation, *Earth Planet. Sci. Lett.*, *199*, 359–372.

Hammond, D. E., J. McManus, W. M. Berelson, C. Meredith, G. P. Klinkhammer, and K. Coale (2000), Diagenetic fractionation of Ge and Si in reducing sediments: The missing Ge sink and a possible mechanism to cause glacial/interglacial variations in oceanic Ge/Si, *Geochim. Cosmochim. Acta*, *64*, 2453–2465.

Hammond, D. E., J. McManus, and W. M. Berelson (2004), Oceanic germanium/silicon ratios: Evaluation of the potential overprint of temperature on weathering signals, *Paleoceanography*, *19*, PA2016, doi:10.1029/2003PA000940.

Hulme, S. M., C. G. Wheat, R. M. Coggon, and J. McManus (2008), Data report: Trace element, Sr isotope, and Ge/Si composition of fluids and sediments in ridge-flank low-temperature hydrothermal environments, in *Juan de Fuca Hydrogeology*, edited by A. T. Fisher et al., *Proc. Integr. Ocean Drill. Program*, doi:10.2204/iodp.proc.301.202.2008.

Hunter, A. G., P. D. Kempton, and P. Greenwood (1999), Low temperature fluid-rock interaction—An isotopic and mineralogical perspective of upper crustal evolution, eastern flank of the Juan de Fuca Ridge (JdFR), ODP Leg 168, *Chem. Geol.*, *155*, 3–28.

Hutnak, M., A. T. Fisher, L. Zühlsdorff, V. Spiess, P. H. Stauffer, and C. W. Gable (2006), Hydrothermal recharge and discharge guided by basement outcrops on 0.7–3.6 Ma seafloor east of the Juan de Fuca Ridge: Observations and numerical models, *Geochem. Geophys. Geosyst.*, *7*, Q07O02, doi:10.1029/2006GC001242.

Hutnak, M., et al. (2007), The thermal state of 18–24 Ma upper lithosphere subducting below the Nicoya Peninsula, northern Costa Rica margin, in *The Seismogenic Zone of Subduction Thrust Faults*, edited by T. Dixon and C. Moore, pp. 86–122, Columbia Univ. Press, New York.

King, S. L., P. N. Froelich, and R. A. Janhke (2000), Early diagenesis of germanium in sediments of the Antarctic South Atlantic: In search of the missing Ge sink, *Geochim. Cosmochim. Acta*, *64*, 1375–1390.

Koga, A. (1967), Germanium, molybdenum, copper and zinc in New Zealand thermal waters, *N. Z. J. Sci.*, *10*, 428–446.

Kolodny, Y., and L. Halicz (1988), The geochemistry of germanium in deep-sea cherts, *Geochim. Cosmochim. Acta*, *52*, 2333–2336.

Kurtz, A. C., L. A. Derry, and O. A. Chadwick (2002), Germanium-silicon fractionation in the weathering environment, *Geochim. Cosmochim. Acta*, *66*, 1525–1537.

Li, Y.-H., and S. Gregory (1974), Diffusion of ions in sea water and in deep-sea sediments, *Geochim. Cosmochim. Acta*, *38*, 703–714.

Lin, H.-L., and C.-J. Chen (2002), A late Pliocene diatom Ge/Si record from the southeast Atlantic, *Mar. Geol.*, *180*, 151–161.

Marescotti, P., D. A. Vanko, and R. Cabella (2000), From oxidizing to reducing alteration: Mineralogical variations in pillow basalts from the east flank, Juan de Fuca Ridge, *Proc. Ocean Drill. Program Sci. Results*, *168*, 119–136.

McManus, J., D. E. Hammond, K. Cummins, G. P. Klinkhammer, and W. M. Berelson (2003), Diagenetic Ge-Si fractionation in continental margin environments: Further evidence for a non-opal Ge sink, *Geochim. Cosmochim. Acta*, *67*, 4545–4557.

Mortlock, R. A., and P. N. Froelich (1996), Determination of germanium by isotope-dilution hydride-generation inductively-coupled mass spectrometry, *Anal. Chim. Acta*, *332*, 645–652.

Mortlock, R. A., P. N. Froelich, R. A. Feely, G. J. Massoth, D. A. Butterfield, and J. E. Lupton (1993), Silica and germanium in Pacific Ocean hydrothermal vents and plumes, *Earth Planet. Sci. Lett.*, *119*, 365–378.

Mottl, M. J., and C. G. Wheat (1994), Hydrothermal circulation through mid-ocean ridge flanks: Fluxes of heat and magnesium, *Geochim. Cosmochim. Acta*, *58*, 2225–2237.

Murray, R. W., D. J. Miller, and K. A. Kryc (2000), Analysis of major and trace elements in rocks, sediments, and interstitial waters by inductively coupled plasma-atomic emission spectrometry (ICP-AES), *Ocean Drill. Program Tech. Note 29*, College Station, Tex.

Pokrovski, G. S., and J. Schott (1998a), Thermodynamic properties of aqueous germanium (IV), hydroxide complexes from 25 to 350°C: Implications for the behavior of Ge and the Ge/Si ratio in hydrothermal fluids, *Geochim. Cosmochim. Acta*, *62*, 1631–1642.

Pokrovski, G. S., and J. Schott (1998b), Experimental study of the complexation of silicon and germanium with aqueous organic species: Implications for Ge and Si transport and the Ge/Si ratio in natural waters, *Geochim. Cosmochim. Acta*, *62*, 3413–3428.

Porter, S., D. A. Vanko, and A. M. Ghazi (2000), Major and trace element compositions of secondary clays in basalts altered at low temperature, eastern flank of the Juan de Fuca Ridge, *Proc. Ocean Drill. Program Sci. Results*, *168*, 149–157.

Robbins, J. M., M. Lyle, and G. R. Heath (1984), A sequential extraction procedure for partitioning elements among coexisting phases in marine sediments, *Coll. Oceanogr. Ref. 84-3*, Oregon State Univ., Corvallis.

Schramm, B., C. W. Devey, K. M. Gillis, and K. Lackschewitz (2005), Quantitative assessment of chemical and mineralogical changes due to progressive low-temperature alteration of East Pacific Rise basalts from 0 to 9 Ma, *Chem. Geol.*, *218*, 281–313.

Scribner, A. M., A. C. Kurtz, and O. A. Chadwick (2006), Germanium sequestration by soil: Targeting the roles of secondary clays and Fe-oxyhydroxides, *Earth Planet. Sci. Lett.*, *243*, 760–770.

Shemesh, A., R. Mortlock, and P. Froelich (1989), Late Cenozoic Ge/Si record of marine biogenic opal: Implications for variations of riverine fluxes to the ocean, *Paleoceanography*, *4*(3), 221–234.

Spinelli, G. A., and M. B. Underwood (2004), Character of sediments entering the Costa Rica subduction zone: Implications for partitioning of water along the plate interface, *Island Arc*, *13*, 432–451.

Spinelli, G., E. Giambalvo, and A. T. Fisher (2004), Hydrologic properties and distribution of sediment, in *Hydrolgeology of the Oceanic Lithosphere*, edited by E. E. Davis, and H. Elderfield, pp. 151–188, Cambridge Univ. Press, Cambridge, U.K.

Stein, C. A., and S. Stein (1994), Constraints on hydrothermal heat flux through the oceanic lithosphere from global heat flow, *J. Geophys. Res.*, *99*, 3081–3095.

Underwood, M., K. D. Hoke, A. T. Fisher, E. R. Giambalvo, E. E. Davis, and L. Zühlsdorff (2005), Provenance, stratigraphic architecture, and hydrogeologic effects of turbidites in northwestern Cascadia Basin, Pacific Ocean, *J. Sediment. Res.*, *75*, 149–174.

Villinger, H., I. Grevemeyer, N. Kaul, J. Hauschold, and M. Pfender (2002), Hydrothermal heat flux through aged oceanic crust: Where does the heat escape?, *Earth Planet. Sci. Lett.*, *202*, 159–170.

Wheat, C. G., and R. E. McDuff (1994), Hydrothermal flow through the Mariana Mounds: Dissolution of amorphous silica and degradation of organic matter on a mid-ocean ridge flank, *Geochim. Cosmochim. Acta*, *58*, 2461–2475.

Wheat, C. G., and J. McManus (2005), The potential role of ridge-flank hydrothermal systems on oceanic germanium and silicon balances, *Geochim. Cosmochim. Acta*, *69*, 2021–2029.

Wheat, C. G., and M. J. Mottl (1994), Hydrothermal circulation, Juan de Fuca Ridge eastern flank: Factors controlling basement water composition, *J. Geophys. Res.*, *99*, 3067–3080.

Wheat, C. G., and J. Tribble (1994), Diagenesis of amorphous silica in Middle Valley, Juan de Fuca Ridge, *Proc. Ocean Drill. Program Sci. Results*, *139*, 341–349.

Wheat, C. G., R. A. Feely, and M. J. Mottl (1996), Phosphate removal by oceanic hydrothermal processes: An update of the phosphate budget of the oceans, *Geochim. Cosmochim. Acta*, *60*, 3593–3608.

Wheat, C. G., H. Elderfield, M. J. Mottl, and C. Monnin (2000), Chemical composition of basement fluids within an oceanic ridge flank: Implications for along-strike and across-strike hydrothermal circulation, *J. Geophys. Res.*, *105*, 13,437–13,447.

Wheat, C. G., M. J. Mottl, and M. Rudniki (2002), Trace element and REE composition of a low-temperature ridge

flank hydrothermal spring, *Geochim. Cosmochim. Acta.*, *66*, 3693–3705.

Wheat, C. G., J. McManus, M. J. Mottl, and E. Giambalvo (2003a), Oceanic phosphorus imbalance: Magnitude of the mid-ocean ridge flank hydrothermal sink, *Geophys. Res. Lett.*, *30*(17), 1895, doi:10.1029/2003GL017318.

Wheat, C. G., H. W. Jannasch, M. Kastner, J. N. Plant, and E. H. DeCarlo (2003b), Seawater transport and reaction in upper oceanic basaltic basement: Chemical data from continuous monitoring of sealed boreholes in a mid-ocean ridge flank environment, *Earth Planet. Sci. Lett.*, *216*, 549–564.

Wheat, C. G., H. W. Jannasch, M. Kastner, J. N. Plant, E. H. DeCarlo, and G. Lebon (2004a), Venting formation fluids from deep-sea boreholes in a ridge flank setting: ODP Sites 1025 and 1026, *Geochem. Geophys. Geosyst.*, *5*, Q08007, doi:10.1029/2004GC000710.

Wheat, C. G., M. J. Mottl, A. T. Fisher, D. Kadko, E. E. Davis, and E. Baker (2004b), Heat flow through a basaltic outcrop on a sedimented young ridge flank, *Geochem. Geophys. Geosyst.*, *5*, Q12006, doi:10.1029/2004GC000700.

Yatabe, A., D. A. Vanko, and A. M. Ghazi (2000), Petrography and chemical compositions of secondary calcite and aragonite in Juan de Fuca Ridge basalts altered at low temperature, *Proc. Ocean Drill. Program Sci. Results*, *168*, 137–148.

Zühlsdorff, L., M. Hutnak, A. T. Fisher, V. Spiess, E. E. Davis, M. Nedimovic, S. Carbotte, H. Villinger, and K. Becker (2005), Site surveys related to IODP Expedition 301: Image-Flux (SO149), and RetroFlux (TN116), expeditions and earlier studies, in *Juan de Fuca Hydrogeology*, edited by A. T. Fisher et al., *Proc. Integr. Ocean Drill. Program*, *301*, doi:10.2204/iodp.proc.301.102.2005.